

# Morphologic Mapping of the Sublingual Microcirculation in Healthy Volunteers

Göksel Güven<sup>a, b, c</sup> Zühre Uz<sup>b</sup> Matthias P. Hilty<sup>d</sup> Burak Bilecenoğlu<sup>e</sup>  
Şakir Akin<sup>f</sup> Yasin Ince<sup>a, b</sup> Can Ince<sup>a</sup>

<sup>a</sup>Department of Intensive Care, Erasmus MC, University Medical Center, Rotterdam, The Netherlands;

<sup>b</sup>Department of Translational Physiology, Amsterdam University Medical Centers, Amsterdam, The Netherlands;

<sup>c</sup>Department of Intensive Care, Hacettepe University, Ankara, Turkey; <sup>d</sup>Institute of Intensive Care, University Hospital of Zurich, Zurich, Switzerland; <sup>e</sup>Department of Anatomy, Ankara Medipol University, Ankara, Turkey; <sup>f</sup>Department of Intensive Care, Hagaziekenhuis Teaching Hospital of The Hague, The Hague, The Netherlands

## Keywords

Microcirculation · Mapping · Sublingual · IDF imaging · Capillary

## Abstract

**Purpose:** Monitoring the sublingual and oral microcirculation (SM-OM) using hand-held vital microscopes (HVMs) has provided valuable insight into the (patho)physiology of diseases. However, the microvascular anatomy in a healthy population has not been adequately described yet. **Methods:** Incident dark field-based HVM imaging was used to visualize the SM-OM. First, the SM was divided into four different fields; Field-a (between incisors-lingua), Field-b (between the canine-first premolar-lingua), Field-c (between the first-second premolar-lingua), Field-d (between the second molar-wisdom teeth-lingua). Second, we investigated the buccal area, lower and upper lip. Total/functional vessel density (TVD/FCD), focus depth (FD), small vessel mean diameters (SVMDs), and capillary tortuosity score (CTS) were compared between the areas. **Results:** Fifteen volunteers with a mean age of  $29 \pm 6$  years were enrolled. No statistical difference was found between the sublingual fields in terms of TVD ( $p = 0.30$ ), FCD ( $p = 0.38$ ), and FD ( $p = 0.09$ ). SVMD was

similar in Field-a, Field-b, and Field-c ( $p = 0.20$ – $0.30$ ), and larger in Field-d ( $p < 0.01$ ,  $p = 0.015$ ). The CTS of the buccal area was higher than in the lips. **Conclusion:** The sublingual area has a homogenous distribution in TVD, FCD, FD, and SVMD. This study can be a description of the normal microvascular anatomy for future researches regarding microcirculatory assessment.

© 2022 The Author(s).

Published by S. Karger AG, Basel

## Introduction

Direct observation of the microcirculation at the bedside provides a unique insight into the pathophysiology of different disease states [1]. Since the introduction of hand-held vital microscopes (HVMs), the relevance of monitoring microcirculation in clinical and preclinical practice, especially in critically ill patients, is increasing [2–4].

Technically, all organ surfaces covered with an epithelial layer are suitable for the microcirculatory assessment using HVM. However, the sublingual microcirculation (SM) is the most frequently used area since it represents an easily accessible window into the human body and has

been found to reflect many diseases [5]. The growing clinical evidence about the importance of monitoring the SM led experts of the Cardiovascular Dynamics Section of the European Society of Intensive Care Medicine to the formulation of guidelines for the assessment of the SM [6]. Based on this consensus, the visualized area should include a mix of venules, capillaries, and, if possible, arterioles. Vessel loops should be avoided since they cause misinterpretations of the analysis because they are considered to belong to a different anatomical region in the mouth.

From an anatomical point of view, the sublingual area is mainly supplied by the lingual artery, which branches off from the external carotid artery. Most of the venous drainage of the sublingual area passes directly to the internal jugular vein via the deep lingual veins. The lymph vessels of the sublingual region drain into the jugulodiaphragmatic group of the deep cervical lymph nodes. The sublingual area has a non-keratinized stratified squamous epithelium, which contains some fat deposits and minor salivary glands in the submucosa layer. The main anatomic structures in the sublingual area are the lingual frenulum in the midline, the sublingual papilla (caruncle) containing the opening of the submandibular salivary ducts, and some of the sublingual salivary ducts; and sublingual folds on either side cover the underlying submandibular ducts and sublingual salivary glands. The SM originates from the same embryogenic origin and displays similar behavior with the splanchnic system [7].

As known from routine sublingual measurements, different microcirculation types and structures exist in the various sublingual area such as the saliva gland, ducts of the glands, areas with vessel loops. Recognition of these structures is crucial for the accurate interpretation of the microvascular parameters since they all have different innervation and blood supply, which might give different reactions to pathological processes. Furthermore, the categorization of the vessel loops could also provide early recognition of chronic diseases such as hypertension, diabetic vasculopathy, and atherosclerotic cardiovascular disease before the appearance of laboratory and clinical symptoms [8, 9].

Description of the normal microvascular anatomy is essential for accurate interpretation of pathologic microvascular findings. However, to our knowledge, no previous study has described the morphological properties of microvessels present in the SM. Although several studies have analyzed the sublingual area of healthy volunteers [3, 10, 11], they focused on only a limited space around the lingual frenulum and have not included other mor-

phological areas in the oral cavity. The present study aims to characterize the morphology of the oral microcirculation (OM) and assess the variability between the healthy population.

## Materials and Methods

This study is a single-center prospective observational study conducted at the Academic Medical Center, Amsterdam University, The Netherlands. Fifteen healthy volunteers aged  $\geq 18$  years were included in the study. The primary objective of the study is to map the morphology of the OM, including the sublingual area, buccal area, and lips. This study was performed using the data of the volunteers' study that was approved by the Medical Ethical Committee of the Academic Medical Center with number W17\_258. All volunteers gave oral informed consent.

### Study Design

Healthy volunteers without symptoms of ongoing diseases such as flu or chronic disease were included in the study. Taking any medication, smoking or being an ex-smoker, and being pregnant were the exclusion criteria. Volunteers were told not to use any product for mouth cleaning and not to have lunch or dinner for at least 2 h before the measurement session. All volunteers were investigated under similar environmental conditions. All measurements were performed in the same room, and sublingual measurements were commenced. Vital signs (body temperature, systemic arterial blood pressure, heart rate, and oxygen saturation) were recorded. The room temperature was monitored and kept constant at  $23^{\circ}\text{C} \pm 1^{\circ}\text{C}$ . Once all the environmental conditions were met and the volunteers had rested for 20 min in a semirecumbent position, three investigators evaluated the microcirculation of the volunteers. The Cytocam-IDF HVM device (Braedius Medical, Huizen, The Netherlands) was used to record SM image sequences. The OM was investigated in two different steps, first the sublingual followed by non-SM. To assess the SM, the sublingual area was divided into four different parts as shown in Figure 1 (a: incisors and lingua, b: canine + first premolar and lingua, c: second premolar + first molar and lingua, and d: second molar + wisdom teeth and lingua). The non-SM included three different regions as the lower lip, upper lip, and buccal area. Measurements were made in 11 different oral areas, as shown in Figure 1.

### Microcirculatory Mapping of the Sublingual Area

The HVM device was covered by a disposable plastic cap and placed on the tissue surface. We recorded five image sequences for each Field-a, -b, -c, and -d. Thus, 20 image sequences were recorded for each volunteer's sublingual area. Once an image sequence was recorded, the HVM device was gently moved to the next area of interest to visualize the different microcirculatory fields. Image recording was performed at a frame rate of 25 frames/s. After that, the images were exported offline for analysis. All sequences were investigated for identification of anatomical structures. The image sequences were stabilized with CCTools 1.7.x and were analyzed in terms of microvessel density (total vessel density [TVD] and functional vessel density [FCD]) using MicroTools [12, 13]. The focus depth (FD) was measured directly using the Cytocam-IDF device (Braedius Medical, Huizen, The Netherlands) during the

study process. Previously, we have validated this method of measuring the FD in biopsy studies obtained from patients [14]. All measurements were started at an FD of 160  $\mu\text{m}$  as a default and then adjusted the FD until the best quality image was obtained. Moreover, the outer tip of the cap was marked with a pen to rule out the presence of an extra space area between the tip of the device and the cap. Two investigators carried out each of the measurements to increase the quality of the recordings. While one investigator was performing the measurement, the other controlled the HVM settings double-checking the camera's position. The MicroTools software measures the small vessel mean diameter (SVMD) individually to allow a quantitative comparison of the microvascular anatomy between the different sublingual regions. Vessel diameter  $\leq 20 \mu\text{m}$  was used to define small vessels. The vessels larger than this diameter are referred to as large vessels. The data were analyzed in a blinded fashion.

#### *Microcirculatory Visualization Using IDF Imaging and Offline Analysis*

Cytocam-IDF (Braedius Medical B.V., Huizen, The Netherlands) uses incident dark-field illumination. Using green light (530 nm) with an isosbestic wavelength for hemoglobin allows visualization of Hb containing red blood cells (RBC) movement in the microcirculation. Therefore, irrespective of the oxygenation of the hemoglobin, RBCs appear as black/gray dots and can be tracked to assess blood flow and calculate the velocity. In addition, a novel stepping motor-assisted focusing mechanism enables precise focusing microvessels by adjusting the FD with 4- $\mu\text{m}$  steps. In this manner, a quantitative measurement of FD is accomplished as well as enabling high-quality point-of-care images. High power light-emitting diodes with rapid pulse time (2 ms) were used for illumination which allows accurate RBC tracking with minimized motion-induced blurring. The IDF imaging device has a full digitalized image and incorporates microscope lenses instead of simple magnification lenses, which provides a view of  $1.55 \times 1.16 \text{ mm}$  that corresponds to a three times larger field of view than previous HVMs. In addition, high-quality lens, high-resolution sensors (between 0.36 and 1.3 megapixels), and automatic and quantitative focusing mechanisms increase contrast and sharpness compared to previous HVM techniques [15]. Image sequences were edited to remove unstable segments, graded for quality, and stabilized using embedded CTools 1.7 software (Braedius Medical B.V., Huizen, The Netherlands). Offline image sequence analysis was then performed using the MicroTools software package that is described in detail elsewhere [12]. This novel software platform consists of an advanced computer vision algorithm that enables the automated quantification of microvessel density and RBC velocity obtained by HVM devices and enables analysis without manual supervision, yielding objective and quantitative results that are not subject to potential operator bias. This software has been recently validated in a large clinical database [13].

#### *Microvascular Parameters*

TVD of vessels  $< 20 \mu\text{m}$  is expressed as TVD, which is calculated as the ratio of the length of the microvessels to the total field of view ( $\text{TVD} = \text{length of the microvessels} / \text{total surface area of the field of view}$ ). FCD is defined as the sum of the length of the microvessels containing moving RBCs divided by the total surface area of the field of view. SVMD is defined as the diameter of a microvessel. The FD is the distance between the surfaces of the tissue

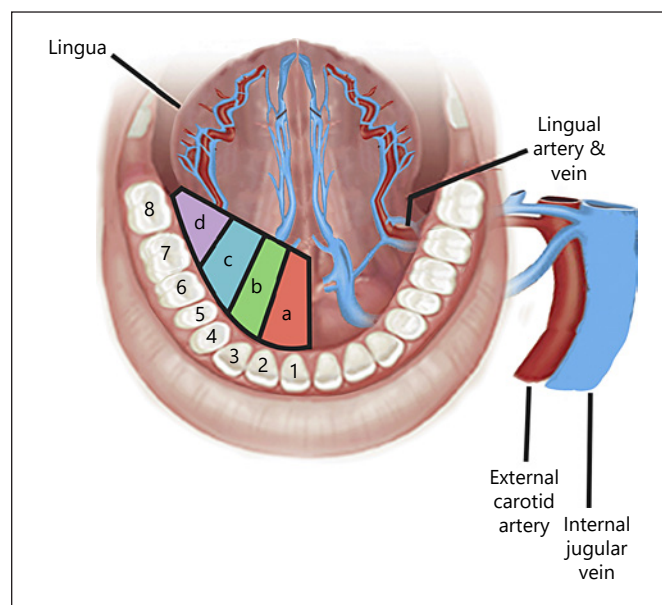


**Fig. 1.** Mapping of the SM. Macrovascular anatomy and mapping of SM are shown in the figure. The sublingual area is mainly supplied and drained by the lingual artery and deep lingual veins, which are branches of the external carotid artery and internal jugular vein, respectively. The sublingual area is divided into four different parts to map the SM, as shown in the figure. Field-a displays the area between the incisors (1 and 2) and the lingua. Field-b displays the area between the Canine + first premolar (3 and 4) and the lingua. Field-c displays the area between the second premolar + first molar (5 and 6) and the lingua and Field-d displays the area between the second molar + wisdom teeth (7 and 8) and the lingua. The same four fields exist on the other side of the sublingual area.

to the plane containing the microvessels. FD value was directly recorded from the machine.

#### *The Capillary Tortuosity Score*

The Capillary Tortuosity Score (CTS) describes the morphological architecture of capillaries based on the number of twists per capillary [8]. The number of twists among the majority of the capillaries defines the score and varies from pinhead twists to four twists (Score 0: no twists, Score 1: one twist, Score 2: two twists, Score 3: three twists, Score 4: four twists) (Fig. 2). This score has been shown to have a good inter- and intraobserver variability [8].

#### *Statistics*

The Shapiro-Wilk test was used to assess if the data were distributed normally. All values were displayed as the mean  $\pm$  standard deviation or median with an interquartile range if the data were distributed skewed or nonskewed, respectively. Since each group's values were shown to have a nonskewed distribution, a nonparametric test (the Friedman test) was performed to analyze these data. Per-vessel diameter distributions measured by MicroTools were compared between different sublingual fields using linear mixed model analysis [16]. The sublingual field was entered

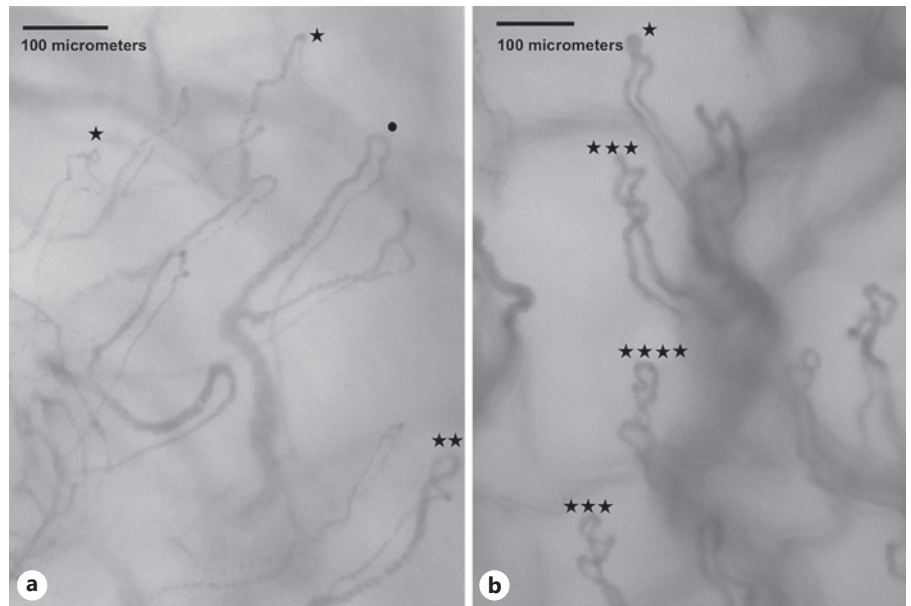


**Fig. 2.** The CTS is defined as the number of capillary twists in the majority of capillaries existing in the field of view. The figure shows capillary images where each star and dot indicates the presence of twists present in a capillary loop (**a** displays no twist, one twist, and two twists, **b** includes three and four twists) (black dot, no twist; one star, one twist; two stars, two twists; three stars, three twists; four stars, four twists).

into the model as fixed effects, and individual intercepts for subjects and per-subject random slopes representing the effect on the dependent variables were entered as random effects.  $p$  values were calculated using a likelihood ratio test of the full model with the effect in question against a “null model” that lacks the effect in question [17].  $p$  values for individual fixed effects were obtained via the Satterthwaite approximation [18]. A two-sided  $p$  value  $<0.05$  was considered as a criterion for significance. All the statistical tests were performed within the R environment for statistical computing, version 3.4.2 (R Foundation for Statistical Computing, Vienna, Austria; <http://www.R-project.org/>), and the figures were created with the ggplot2 software package, version 2.2.1.

## Results

The mean age of the 15 volunteers was  $29 \pm 6$  years (range 22–39 years; 12 men, 3 women). The mean age of the volunteers was  $30 \pm 6$  (range 23–39 years) for the men and  $26 \pm 6$  (range 22–3 years), respectively, ( $p = 0.47$ ) for the women. None of the volunteers had active disease or comorbidity. Oral microcirculatory measurements were performed with the same device and were well tolerated by all volunteers.

### Sublingual Microcirculatory Parameters

Three hundred image sequences from the 15 volunteers were measured using MicroTools to yield TVD, FCD, SVMd, and FD of the different sublingual microcirculatory fields. There were around 40,000 frames used to evaluate different kinds of structures and microvascu-

lar types within different regions. Thirty-four image sequences (about 5,000 frames) were excluded due to low image quality.

TVD was examined separately in small and large microvessels and presented as small vessel TVD and large vessel TVD using a cutoff value of  $20 \mu\text{m}$  diameter for classification. Small vessel TVD was found to be  $20.9$  (IQR,  $20.5\text{--}23.1$ )  $\text{mm}/\text{mm}^2$  in Field-a,  $22.2$  (IQR,  $21.5\text{--}24.5$ )  $\text{mm}/\text{mm}^2$  in Field-b,  $23.1$  (IQR,  $21.7\text{--}24.5$ )  $\text{mm}/\text{mm}^2$  in Field-c, and  $21.6$  (IQR,  $19.7\text{--}23.0$ )  $\text{mm}/\text{mm}^2$  in Field-d ( $p = 0.30$ ) (Fig. 3; Table 1). Large vessel TVD was  $7.6$  (IQR,  $6.6\text{--}8.5$ )  $\text{mm}/\text{mm}^2$  in Field-a,  $7.2$  (IQR,  $6.8\text{--}7.9$ )  $\text{mm}/\text{mm}^2$  in Field-b,  $7.3$  (IQR,  $6.6\text{--}7.6$ )  $\text{mm}/\text{mm}^2$  in Field-c,  $7.9$  (IQR,  $7.4\text{--}8.6$ )  $\text{mm}/\text{mm}^2$  in Field-d ( $p = 0.11$ ) (Fig. 3; Table 1). There was no statistical difference between the different regions in terms of small, large or total microvessel density. The coefficient of variance of small vessel TVD was found to be 11.6%, 10.1%, 9.6%, 10% in the Field-a, Field-b, Field-c, and Field-d, respectively. The FCD of small microvessels were  $20.0$  (IQR,  $19.7\text{--}22.7$ )  $\text{mm}/\text{mm}^2$  at Field-a,  $21.6$  (IQR,  $20.6\text{--}23.7$ )  $\text{mm}/\text{mm}^2$  at Field-b,  $22.4$  (IQR,  $21.1\text{--}23.4$ )  $\text{mm}/\text{mm}^2$  at Field-c,  $21.2$  (IQR,  $19.3\text{--}22.3$ )  $\text{mm}/\text{mm}^2$  at Field-d ( $p = 0.38$ ) (Fig. 3; Table 1). The FD had a trend to be deeper at Field-b but was not statistically different between different regions ( $160$  [IQR,  $141\text{--}210$ ]  $\mu\text{m}$  in Field-a,  $177$  [IQR,  $101\text{--}186$ ]  $\mu\text{m}$  in Field-b,  $160$  [IQR,  $116\text{--}201$ ]  $\mu\text{m}$  in Field-c,  $170$  [IQR,  $110\text{--}195$ ]  $\mu\text{m}$  in Field-d,  $p = 0.09$ ) (Fig. 3; Table 1). In addition, microcirculatory parameters were compared

**Fig. 3.** Box-Plots of microcirculatory parameters within different mouth regions. Microcirculatory parameters were assessed for homogeneity among sublingual fields. The analyses were performed on the complete data set of the 15 healthy volunteers. Friedman test was used for the statistical analysis. No statistical significance was found between the defined sublingual fields for the distribution of small vessel TVD ( $p = 0.30$ ), large vessel TVD ( $p = 0.11$ ), FCD ( $p = 0.38$ ), and FD ( $p = 0.09$ ). Red, green, blue, and purple bars displayed Field-a, -b, -c, and -d, respectively. TVD, total vessel density; FCD, functional capillary density; mm, millimeter.

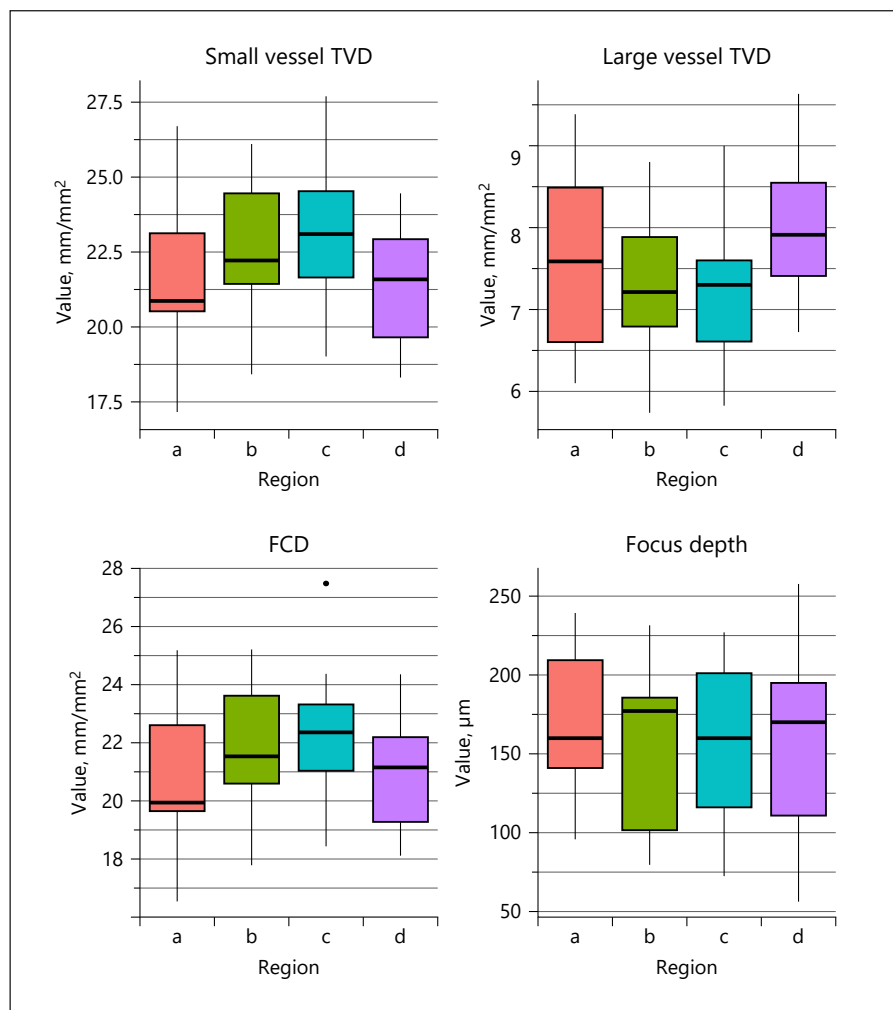


**Table 1.** Microvascular parameters of the different sublingual fields

Field	Small vessel TVD Median (IQR), mm/mm <sup>2</sup>	Large vessel TVD Median (IQR), mm/mm <sup>2</sup>	FCD Median (IQR), mm/mm <sup>2</sup>	FD Median (IQR), µm
a	20.9 (20.5–23.1)	7.6 (6.6–8.5)	20.0 (19.7–22.7)	160 (141–210)
b	22.2 (21.5–24.5)	7.2 (6.8–7.9)	21.6 (20.6–23.7)	177 (101–186)
c	23.1 (21.7–24.5)	7.3 (6.6–7.6)	22.4 (21.1–23.4)	160 (116–201)
d	21.6 (19.7–23.0)	7.9 (7.4–8.6)	21.2 (19.3–22.3)	170 (110–195)
<i>p</i> value	0.30	0.11	0.38	0.09

Sublingual microcirculatory parameters, including small vessel TVD, large vessel TVD, FCD, and FD, were analyzed in all fields. We used Cytocam-IDF (Braedius Medical B.V., Huizen, The Netherlands) to visualize the microcirculation and included fifteen healthy volunteers' image sequences. Statistical analyses were performed using Friedman Test due to the skewed distribution was found using the Shapiro-Wilk test. Values were displayed as the median (before parenthesis) and interquartile range (in the parenthesis). No statistical significance was found between the defined sublingual fields for the distribution of small vessel TVD ( $p = 0.30$ ), large vessel TVD ( $p = 0.11$ ), FCD ( $p = 0.38$ ), and FD ( $p = 0.09$ ). TVD, total vessel density; FCD, functional capillary density; mm, millimeter; µm, micrometer.

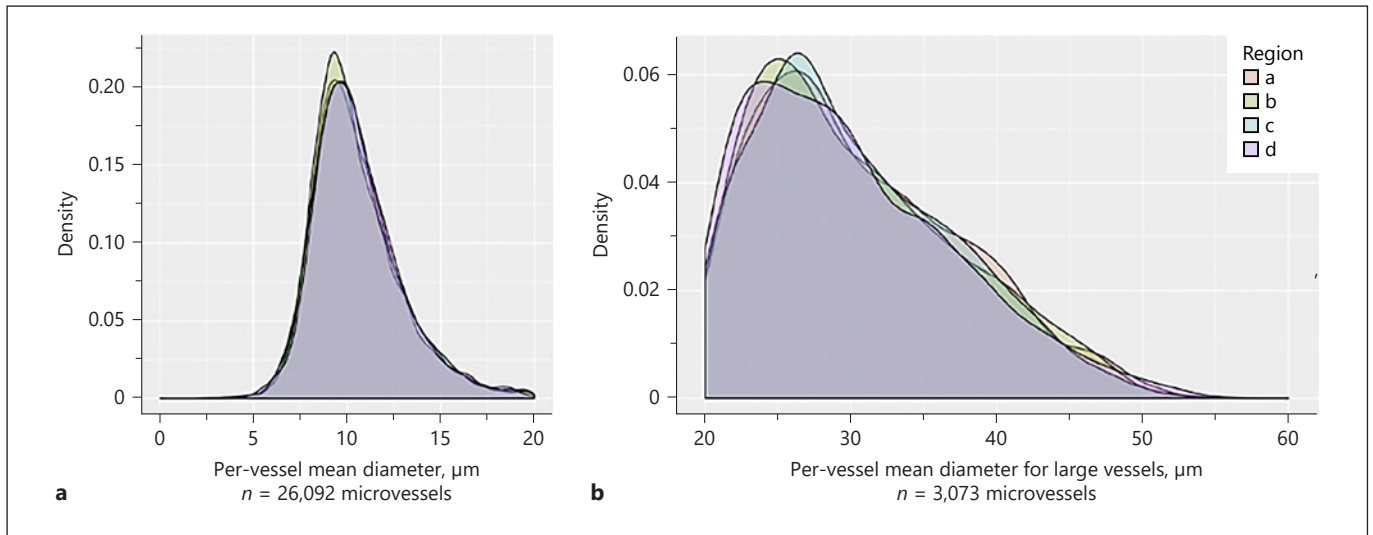


**Fig. 4. a, b** Individual microvascular diameter distributions in the different sublingual regions. SVMDs are defined as the horizontal diameter of the vessels. About 26,092 microvessels and 3,073 macro vessels were detected among 266 image sequences. Per-vessel diameter distributions measured by MicroTools were compared between different sublingual regions using linear mixed model analysis. SVMDs were found similar in Field-a, -b, and -c ( $10.51 \pm$

$2.37$ ,  $10.47 \pm 2.35$ , and  $10.55 \pm 2.37$  mm, respectively, individual fixed effect  $p = 0.20-0.30$ ), and larger in Field-d ( $10.61 \pm 2.35$  mm, overall  $p < 0.01$ , individual fixed effect  $p$  for Field-d = 0.015). There was no difference between sublingual regions for large vessel mean diameters (overall  $30.35 \pm 6.99$  mm,  $p = 0.43$ ). Red, green, blue, and purple density plots displayed Field-a, -b, -c, and -d, respectively.  $n$ , number of microvessels.

**Table 2.** Comparison of CTSs between upper and lower lips and buccal area

CTS	Lower lip <sup>*,#</sup>	Upper lip <sup>*,†</sup>	Buccal area <sup>#,†</sup>
0: no twists	5	5	2
1: 1 twist	9	7	6
2: 2 twists	1	2	5
3: 3 twists	0	1	1
4: 4 or more twists	0	0	1

CTS is a microvascular score that morphologically assesses microvascular architecture based on the number of twists per capillary (Fig. 2). The table shows the number of volunteers that have the CTS in the right column. The volunteers predominantly have CTS-1 at the lower lip, upper lip, and buccal area, as displayed at the table. The CTS was not statistically different between the lower and upper lip ( $p = 0.5$ ). However, CTS was much higher in the buccal area than lower lip ( $p = 0.01$ ) and upper lip ( $p = 0.03$ ). CTS, capillary tortuosity score. \*  $p = 0.5$ . #  $p = 0.01$ . †  $p = 0.03$ .

between men and women in all sublingual fields. However, there was no statistical difference in TVD, FCD, and FD between men and women (data were not shown).

SVMDs were similar in Field-a, -b, and -c ( $10.51 \pm 2.37$ ,  $10.47 \pm 2.35$ , and  $10.55 \pm 2.37$   $\mu\text{m}$ , respectively, in-

dividual fixed effect  $p = 0.20-0.30$ ), and larger in Field-d ( $10.61 \pm 2.35$   $\mu\text{m}$ , overall  $p < 0.01$ , individual fixed effect  $p$  for Field-d = 0.015) (Fig. 4). No difference between sublingual fields was found for large vessel mean diameters ( $30.35 \pm 6.99$   $\mu\text{m}$ ,  $p = 0.43$ ).

The morphology of the microcirculation of all volunteers was evaluated in terms of microvessel structure in the upper and lower lip and in the buccal areas. The CTS was used for scoring the morphology of the capillaries (Table 2). Each number in Table 2 corresponds to the number of volunteers that had the same subscore. There was no difference between the upper and lower lip ( $p = 0.5$ ). However, the CTS was higher in the buccal area compared to both upper and lower lip ( $p = 0.03$  and  $p = 0.01$ , respectively) (Table 2).

## Discussion

To the best of our knowledge, this study is the first to quantitatively assess the morphological structures of the complete OM using the latest generation IDF imaging HVM. The use of improved optics of the latest generation IDF imaging for characterizing baseline values of healthy humans is important because several studies have shown

higher microvascular densities in human volunteers than those found using the previous generation sidestream dark-field (SDF) imaging devices [15, 19]. For example, Kannoore Edul et al. [9], using SDF imaging found in volunteers a sublingual microcirculatory density of 16.9 mm/mm<sup>2</sup>, whereas in this study, we found a density of 20.9 mm/mm<sup>2</sup> similar to found in other studies using IDF imaging. Furthermore, the present study describes ranges of the microvascular parameters throughout the oral field, unlike previous studies where precise anatomical locations of the measurements were lacking. Moreover, FD and quantitative distribution of SVMs within the whole sublingual field are reported for the first time in a healthy human population. We found that all fields of the sublingual area have similar microvessel density regardless of the presence of vessel loops in the field of interest. The distance between the surface of the tissue and the microvessels was found to be between 160 and 170 μm. The mean diameter of small vessels was found to be larger in the back of the mouth compared to other locations.

The morphological mapping of the normal SM is of importance because the sublingual location is by far the most studied microcirculatory location in patients having different states of disease, especially in critically ill patients [3, 20]. Point-of-care assessment of the microvessel density and microvascular flow parameters can potentially provide valuable information regarding the diffusive and convective capacity of oxygen transport of the microcirculation [21, 22]. Similarly, chronic systemic diseases such as diabetes mellitus, hypertension, coronary artery disease have shown to be associated with sublingual microvascular alterations [9, 23, 24]. However, it is unknown whether early recognition of microvascular abnormality with HVM can predict microvascular complications before developing macrovascular and/or clinical complications. Identifying the extent of microcirculatory alterations as a marker of disease can only be accomplished if there is knowledge regarding the baseline characteristics of the microvessels under conditions of health.

In the current study, the SM revealed a morphologically heterogeneous capillary pattern. Firstly, the sublingual field showed the presence of more capillary loops toward to backside of the mouth (Fields c and d). Also, more capillary loops were found near the sublingual fold. This is probably due to the anatomical location of the sublingual saliva glands, which are present under the sublingual folds [25]. Identifying the presence of vessel-loop free fields is crucial for sublingual monitoring since an area without the presence of capillary loops is required for the microcirculatory assessment with an HVM [6]. A sec-

ond finding was that the FD of the microcirculation did not significantly differ between the sublingual regions even though heterogeneity within the volunteers was present. Each volunteer had his or her characteristic focal depth. However, considering all patient measurements, the average distance between the SM and the tissue surface was found around 160 μm. Similarly, Ten Tusscher et al. [26] reported an FD of around 130 μm [22]. The purpose of their study was to identify if this variable was related to tissue edema; however, they found that there was no correlation between the severity of tissue edema and FD [26]. On the other hand, this parameter has been shown to identify the presence of vaginal atrophy in a quantitative manner. In a validation study using vaginal biopsies, Kastelein et al. [14] found a linear correlation between histologically determined focal depth and that measured using IDF imaging. Using this methodology, Weber et al. [27, 28] showed how successful estrogen treatment in patients could be demonstrated by changes in FD in patients suffering from vaginal atrophy [14].

Only a few studies have been performed describing the anatomical structure of the OM [29, 30]. These researches mainly focused on the lip, gingiva, and buccal microvessels due to the technical limitations to reach the sublingual area [29, 30]. However, these studies used previous video-capillaroscopy techniques the values of which have been shown to deviate from the newly introduced HVM [15, 19, 31, 32]. Hubble et al. [11] showed the normal ranges of sublingual microvessel diameters with the second-generation SDF imaging handheld video microscope and visualized the microvessels in a limited sublingual field. In contrast, our study used the latest generation HVM (Cytocam-IDF) to comprehensively map the whole OM. This device has already been validated (for labial capillaries [8]) and confirmed to have a sublingual image with higher quality and visualize more capillaries (30% more vessels) than its predecessors [15, 19]. For example, Kannoore Edul et al. [33] found, using SDF imaging, sublingual microcirculatory densities in human volunteers of 16.9 mm/mm<sup>2</sup>, whereas our study found a density of 20.9 mm/mm<sup>2</sup> similar to that found in other studies using IDF imaging. Moreover, the novel full automated and validated software program MicroTools was used for data analysis. This innovative software enables rapid data analysis and is expected to start a new era on the bedside microcirculatory-based diagnosis and treatment modalities in the future. Importantly, we believe that the current study enabled a base for future studies by comprehensively providing normal ranges and anatomical structure of the microvessels.

In this study, TVD and FCD were found 20–21  $\mu\text{m}/\text{mm}^2$  and were not significantly different between the sublingual regions. This finding is important because it allows a random choice for the best sublingual area conforming to the Massey Microcirculation Image Quality Score [34]. Previous studies were also reported a compatible TVD range in a healthy population [9, 11, 15, 35]. Moreover, the area between the incisors' teeth, lingua, and frenulum (as depicted Field-a) was found to be the most suitable area in most of the volunteers. As recommended in the consensus report [6] and the Massey Microcirculation Image Quality Score [34], this field was determined to contain the least capillary loops among the sublingual area. This finding confirms the location that Uz et al. [36] previously described as the triangle area.

International guidelines recommend visualizing a minimum of 3–5 image sequences for a sublingual measurement to be acceptable [6, 37]. However, the guidelines also recommend visualizing the same spot to monitor the changes in the same field [6]. Practically, this is hard to realize as the probe can easily move. The sublingual map generated in this study could help the observer to find a previously visualized spot by identifying its location on the map (such as aR [Field-a, right side] and aL [Field-a, left side]).

Another finding of the current study was defining the number of capillary tortuosities, which has been proposed as a useful parameter for recognizing microvascular alterations in patients with chronic diseases such as diabetes [8]. In previous studies, normal ranges of capillary tortuosity were found between 0 and 2 [8, 29], which agreed with our findings of values between 0 and 1. The CTS was not different between the upper and lower lip. However, our study showed that the buccal area showed a significantly higher CTS than the lips. An important correlation was reported between smoking and capillary tortuosity [38]. In addition, Djaberi et al. [8] reported that the high CTS (0–2) is significantly associated with higher obstructive coronary artery disease in asymptomatic diabetic patients.

The current study has several limitations. The relatively small number of volunteers, notably women, concerns that the findings may not be generalized to larger populations. However, the number of subjects we investigated is similar to previous volunteer studies, which aimed to examine the sublingual parameters [3, 10, 11]. Confounding factors such as the choice of ethnicity may also affect the quantitative value of the variables measured [39]. Certain chronic diseases and older age may also affect the

nature of the morphology and density of the microcirculatory structure. Finally, the participants of the current study are relatively younger, and microcirculatory parameters might change by age. Future studies would have to investigate the values of the microcirculatory variables identified in this study in the older volunteers and the patients. Finally, a comparison of these baseline values to states of disease may have been undertaken. However, this would have been a considerable undertaking which we leave for future studies since each specific state of disease has deviation in specific types of microcirculatory values as we and others have shown in previous studies [13].

## Conclusion

The sublingual area has a homogenous distribution in small and large vessel TVD, small and large vessel FCD, and FD. The lateral sublingual region, between the second molar, wisdom teeth, and lingua, was found to possess larger individual vessels. Therefore, based on the current finding, investigators could use the area between the incisors and the lingua for measurements for obtaining reproducible measurements of the SM in clinical studies.

## Statement of Ethics

All procedures performed in studies involving human participants were under the ethical standards of the institutional and/or national research committee and with the 1964 Helsinki Declaration and its later amendments or comparable ethical standards. As stated in the text, it is approved by the Medical Ethical Committee of the Academic Medical Center with number W17\_258.

## Conflict of Interest Statement

Dr. Ince developed the SDF, the handheld video microscope and is listed as the inventor on related patents commercialized by MicroVision Medical under a license from the Academic Medical Center. He receives no royalties or benefits from this license. He has been a consultant for MicroVision Medical in the past but has not been involved with this company for more than 5 years now and holds no shares or stock. Braedius Medical, a company owned by a relative of Dr. Ince, developed and designed a handheld microscope called CytoCam-Incident Dark Field imaging that was used in this study, but Dr. Ince has no financial relationship with Braedius Medical, that is, never owned shares or received consultancy or speaker fees from Braedius Medical. An internet site called [microcirculationacademy.com](http://microcirculationacademy.com).

org offers educational courses and services related to clinical microcirculation and provides access to MicroTools. The site is run by Active Medical BV of which Dr. Ince is a shareholder and Dr. Hilty has received financial support regarding MicroTools. The remaining authors have disclosed that they do not have any potential conflicts of interest.

## Funding Sources

The authors have no funding source to declare.

## References

- 1 Ince C. Hemodynamic coherence and the rationale for monitoring the microcirculation. *Crit Care*. 2015 Dec;19 Suppl 3(Suppl 3):S8.
- 2 Mathura KR, Bouma GJ, Ince C. Abnormal microcirculation in brain tumours during surgery. *Lancet*. 2001 Nov;358(9294):1698–9.
- 3 De Backer D, Creteur J, Preiser JC, Dubois MJ, Vincent JL. Microvascular blood flow is altered in patients with sepsis. *Am J Respir Crit Care Med*. 2002 Jul;166(1):98–104.
- 4 De Backer D, Donadello K, Sakr Y, Ospina-Tascon G, Salgado D, Scolletta S, et al. Microcirculatory alterations in patients with severe sepsis: impact of time of assessment and relationship with outcome\*. *Crit Care Med*. 2013 Mar;41(3):791–9.
- 5 Cerny V. Sublingual microcirculation. *Appl Cardiopulm Pathophysiol*. 2012;16:229–48.
- 6 Ince C, Boerma EC, Cecconi M, De Backer D, Shapiro NI, Duranteau J, et al. Second consensus on the assessment of sublingual microcirculation in critically ill patients: results from a task force of the European Society of Intensive Care Medicine. *Intensive Care Med*. 2018 Mar;44(3):281–99.
- 7 Standing S. *Gray's anatomy: the anatomical basis of clinical practice*. 41st ed. Elsevier; 2016.
- 8 Djaberi R, Schuijff JD, de Koning EJ, Wijewickrama DC, Pereira AM, Smit JW, et al. Non-invasive assessment of microcirculation by sidestream dark field imaging as a marker of coronary artery disease in diabetes. *Diabetes Vasc Dis Res*. 2013 Mar;10(2):123–34.
- 9 Kanoore Edul VS, Ince C, Estenssoro E, Ferrara G, Arzani Y, Salvatori C, et al. The effects of arterial hypertension and age on the sublingual microcirculation of healthy volunteers and outpatients with cardiovascular risk factors. *Microcirculation*. 2015 Aug;22(6):485–92.
- 10 Orbegozo Cortés D, Puflea F, Donadello K, Taccone FS, Gottin L, Creteur J, et al. Normobaric hyperoxia alters the microcirculation in healthy volunteers. *Microvasc Res*. 2015 Mar; 98:23–8.
- 11 Hubble SM, Kyte HL, Gooding K, Shore AC. Variability in sublingual microvessel density and flow measurements in healthy volunteers. *Microcirculation*. 2009 Jan;16(2):183–91.
- 12 Hilty MP, Guerci P, Ince Y, Toraman F, Ince C. MicroTools enables automated quantification of capillary density and red blood cell velocity in handheld vital microscopy. *Commun Biol*. 2019 Dec;2(1):217.
- 13 Hilty MP, Akin S, Boerma C, Donati A, Erdem Ö, Giaccaglia P, et al. Automated algorithm analysis of sublingual microcirculation in an international multicenter database identifies alterations associated with disease and mechanism of resuscitation. *Crit Care Med*. 2020;48(10). Available from: [https://journals.lww.com/ccmjournal/Fulltext/2020/10000/Automated\\_Algorithm\\_Analysis\\_of\\_Sublingual.29.aspx](https://journals.lww.com/ccmjournal/Fulltext/2020/10000/Automated_Algorithm_Analysis_of_Sublingual.29.aspx).
- 14 Kastelein AW, Diedrich CM, Jansen CHJR, Zwolsman SE, Ince C, Roovers JWR. Validation of noninvasive focal depth measurements to determine epithelial thickness of the vaginal wall. *Menopause*. 2019 Oct;26(10): 1160–5.
- 15 Aykut G, Veenstra G, Scorcella C, Ince C, Boerma C. Cytocam-IDF (incident dark field illumination) imaging for bedside monitoring of the microcirculation. *Intensive Care Med Exp*. 2015 Dec;3(1):40.
- 16 Bates D, Mächler M, Bolker B, Walker S. Fitting linear mixed-effects models Using lme4. *J Stat Soft*. 2015 [cited 2020 Dec 21];67(1).
- 17 Baayen RH, Davidson DJ, Bates DM. Mixed-effects modeling with crossed random effects for subjects and items. *J Mem Lang*. 2008 Nov; 59(4):390–412.
- 18 Barr DJ, Levy R, Scheepers C, Tily HJ. Random effects structure for confirmatory hypothesis testing: keep it maximal. *J Mem Lang*. 2013 Apr;68(3):255–78.
- 19 van Elteren HA, Ince C, Tibboel D, Reiss IK, de Jonge RC. Cutaneous microcirculation in preterm neonates: comparison between sidestream dark field (SDF) and incident dark field (IDF) imaging. *J Clin Monit Comput*. 2015 Oct;29(5):543–8.
- 20 De Backer D, Creteur J, Dubois MJ, Sakr Y, Vincent JL. Microvascular alterations in patients with acute severe heart failure and cardiogenic shock. *Am Heart J*. 2004 Jan;147(1): 91–9.
- 21 Ince C, Mik EG. Microcirculatory and mitochondrial hypoxia in sepsis, shock, and resuscitation. *J Appl Physiol*. 2016 Jan 15;120(2): 226–35.
- 22 Kara A, Akin S, Ince C. Monitoring microcirculation in critical illness. *Curr Opin Crit Care*. 2016 Oct;22(5):444–52.
- 23 Junqueira CLC, Magalhães MEC, Brandão AA, Ferreira E, Cyrino FZGA, Maranhão PA, et al. Microcirculation and biomarkers in patients with resistant or mild-to-moderate hypertension: a cross-sectional study. *Hypertens Res*. 2018 Jul;41(7):515–23.
- 24 den Uil CA, Lagrand WK, van der Ent M, Jewbali LSD, Cheng JM, Spronk PE, et al. Impaired microcirculation predicts poor outcome of patients with acute myocardial infarction complicated by cardiogenic shock. *Eur Heart J*. 2010 Dec;31(24):3032–9.
- 25 Holsinger FC, Bui DT. Anatomy, function, and evaluation of the salivary glands. In: Myers EN, Ferris RL, editors. *Salivary gland disorders*. Berlin, Heidelberg: Springer Berlin Heidelberg; 2007. p. 1–16 [cited 2020 Nov 1]. Available from: [http://link.springer.com/10.1007/978-3-540-47072-4\\_1](http://link.springer.com/10.1007/978-3-540-47072-4_1).
- 26 Ten Tusscher B, Gudden C, van Vliet S, Smit B, Ince C, Boerma EC, et al. Focus on focus: lack of coherence between systemic and microvascular indices of oedema formation. *Anaesthesiol Intensive Ther*. 2017;49:350–7.
- 27 Weber MA, Milstein DMJ, Ince C, Rengerink KO, Roovers J-PWR. Vaginal microcirculation: non-invasive anatomical examination of the micro-vessel architecture, tortuosity and capillary density. *Neurourol Urodyn*. 2015 Nov;34(8):723–9.
- 28 Weber MA, Diedrich CM, Ince C, Roovers JP. Focal depth measurements of the vaginal wall: a new method to noninvasively quantify vaginal wall thickness in the diagnosis and treatment of vaginal atrophy. *Menopause*. 2016 Aug;23(8):833–8.

## Author Contributions

G.G.: and C.I. study design; G.G., S.A., and Y.I.: data analysis; G.G. and B.B.: writing the paper; G.G., C.I., Z.U., and B.B.: revising the paper; and G.G. and Y.I.: conducting the study and collecting data. All the authors read and approved the manuscript.

## Data Availability Statement

The authors will make the data available upon request to the authors (c.ince@erasmusmc.nl).

- 29 Giuseppe Alessandro S, Antonino C, Messina P. Anatomical evaluation of oral microcirculation: capillary characteristics associated with sex or age group. *Ann Anat*. 2009 Jan; 191(4):371–8.
- 30 Scardina GA, Messina P. Oral microcirculation in post-menopause: a possible correlation with periodontitis. *Gerodontology*. 2012 Jun;29(2):e1045–51.
- 31 Goedhart PT, Khalilzada M, Bezemer R, Merza J, Ince C. Sidestream dark field (SDF) imaging: a novel stroboscopic LED ring-based imaging modality for clinical assessment of the microcirculation. *Opt Express*. 2007 Nov 12; 15(23):15101–14.
- 32 Mathura KR, Vollebregt KC, Boer K, De Graaff JC, Ubbink DT, Ince C. Comparison of OPS imaging and conventional capillary microscopy to study the human microcirculation. *J Appl Physiol*. 2001 Jul 1;91(1):74–8.
- 33 Kanoore Edul VS, Enrico C, Laviolle B, Risso Vazquez A, Ince C, Dubin A. Quantitative assessment of the microcirculation in healthy volunteers and in patients with septic shock\*. *Crit Care Med*. 2012 May;40(5):1443–8.
- 34 Massey MJ, LaRochelle E, Najarro G, Karmacharla A, Arnold R, Trzeciak S, et al. The microcirculation image quality score: development and preliminary evaluation of a proposed approach to grading quality of image acquisition for bedside videomicroscopy. *J Crit Care*. 2013 Dec;28(6):913–7.
- 35 Favaron E, Ince C, Hilty MP, Ergin B, van der Zee P, Uz Z, et al. Capillary leukocytes, microaggregates, and the response to hypoxemia in the microcirculation of coronavirus disease 2019 patients. *Crit Care Med*. 2021 Apr 1; 49(4):661–70.
- 36 Uz Z, Kastelein AW, Milstein DMJ, Liu D, Rassam F, Veelo DP, et al. Intraoperative incident dark field imaging of the human peritoneal microcirculation. *J Vasc Res*. 2018; 55(3):136–43.
- 37 De Backer D, Hollenberg S, Boerma C, Goedhart P, Büchele G, Ospina-Tascon G, et al. How to evaluate the microcirculation: report of a round table conference. *Crit Care*. 2007; 11(5):R101.
- 38 Scardina GA. The effect of cigar smoking on the lingual microcirculation. *Odontology*. 2005 Sep 26;93(1):41–5.
- 39 Gu Y-M, Wang S, Zhang L, Liu Y-P, Thijs L, Petit T, et al. Characteristics and determinants of the sublingual microcirculation in populations of different ethnicity. *Hypertension*. 2015 May;65(5):993–1001.